

Temperature profiles derived from transverse optical shadowgraphy in ultra-intense laser plasma interactions

K. L. Lancaster, J. S. Green, R. G. Evans*,
P. A. Norreys, R. Heathcote,
C. Hernandez-Gomez and I. Musgrave.

Central Laser Facility, STFC, Rutherford Appleton
Laboratory, HSIC, Didcot, Oxon OX11 0QX, UK

J. Pasley**, J. Waugh and N. Woolsey

Department of Physics, University of York,
Heslington, UK

Contact | Kate.Lancaster@stfc.ac.uk

Introduction

One of the goals of many laser plasma experiments investigating electron transport is to determine the temperature as a function of target depth. Looking at the temperature at various positions inside the solid gives an indication of the position of maximum heating and how deep significant target heating can occur. The most common way of determining temperature is to place a buried tracer layer at intervals inside the solid and use X-ray spectroscopy to determine the temperature.

This can be difficult for several reasons. The presence of a buried layer may affect the transport – there are indications from experiments and modeling⁽¹⁾ that buried layers change the way electrons can propagate through the target. This means that the targets employed for transport investigations are changing the very subject of the measurement.

The second problem is that atomic physics can become quite complicated in ultra-intense laser plasma interactions. Many codes used to model this physics assume Maxwellian return currents. Refluxing of electrons mean that the return current has a significant hot component and this must be considered.

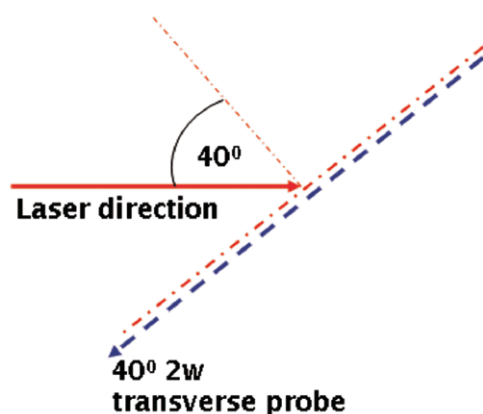


Figure 1. Experimental layout.

P. Koester and L. Gizzi

IPCF-CNR, Pisa, Italy

A. Morace and D. Batani

Universita degli Studi di Milano-Bicocca, Milan, Italy

F. Perez, S. Baton and M. Koenig

LULI, Ecole Polytechnique, Palaiseau, France

*also at Blackett Laboratory, Imperial College, London, UK

**also at Central Laser Facility, STFC, Rutherford Appleton
Laboratory, HSIC, Didcot, Oxon OX11 0QX, UK

In this report, rear surface expansion is measured using transverse optical shadowgraphy. The expansion velocities can be derived from these profiles. We show here that it is possible to derive rear surface temperatures using the expansion velocities in conjunction with a radiation hydrodynamics code to give temperature as a function of target thickness / electron density. We show that the radiation hydrodynamics model alone does not adequately explain the expansion behavior of the thick layered targets and it was necessary to add a simple Rayleigh-Taylor model to produce more realistic temperatures.

Experimental setup

In this experiment a variety of targets were irradiated. This report focuses mainly on thick slabs of SiO₂ and Al, 25 μm and 50 μm thick with 1 μm Cu layers on the rear side for Cu Kα imaging. Small (400 × 400 μm), thin (~4 μm total), layered targets of CH/X/CH, SiO₂/X/CH, and Al/X/CH were used where X is a tracer layer of Ni or Al.

The experiment was conducted in Vulcan TAP, the beam of which was delivering ~440 J onto the gratings, in a ~600 fs pulse. The focal spot was 6 × 4 μm and the intensity was ~6.4 × 10²⁰ W/cm².

A suite of diagnostics was employed to measure various aspects of the interaction. Optical diagnostics included transverse optical shadowgraphy, and rear side optical emission imaging (specifically optical transition radiation). X-ray diagnostics included X-ray pinhole imaging, Cu Kα imaging with a spherical crystal, and a mica crystal spectrometer.

The expansion on the front and back surfaces of the target was diagnosed using a transverse optical probe. The 1.054 μm light was frequency doubled to 527 nm using a KDP crystal. The pulse length of the probe and main interaction beam were identical and synchronisation of the beams was performed using an optical streak camera.

The shadowgraphy images were recorded 200 ps after the interaction using an 8-bit CCD camera connected to a personal computer via image acquisition software. The

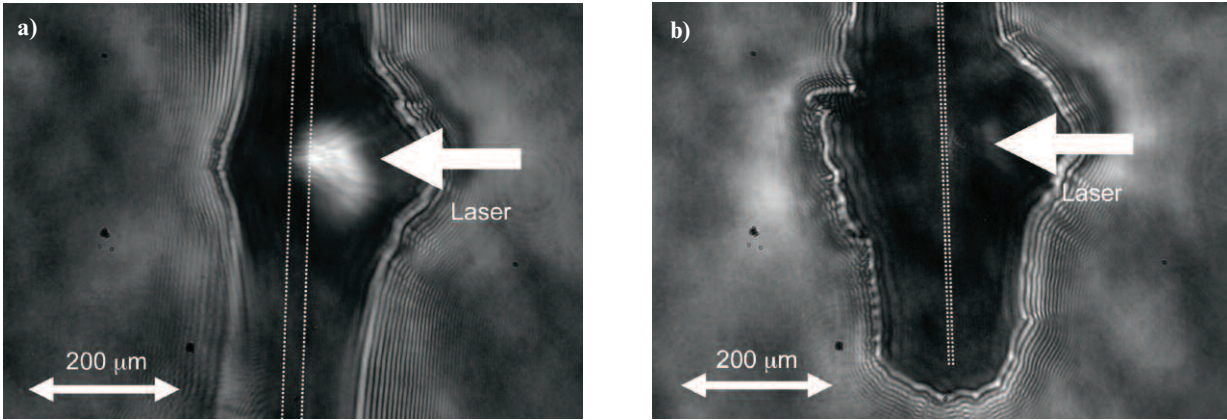


Figure 2. a) Shadowgraph of 25 μm SiO₂ + 1 μm Cu back layer taken at $t_0 + 200$ ps, b) Shadowgraph of 4 μm Al / 1 μm Ni / 1 μm CH taken at $t_0 + 200$ ps. The dotted lines mark the position of the original target surfaces.

magnification was 8.5 and the f number was 4.5. The resolution of the probe system was found to be ~4 μm. Interferograms were taken previously, using a Normarski interferometer and a 16 bit Andor technology CCD camera. Analysis of these interferograms shows a cutoff density of $5 \times 10^{19} \text{ cm}^{-3}$.

Results

Shadowgrams were recorded for a wide range of target types. Figure 2a and b show two typical examples of shadowgrams for thick and thin targets. Figure 2a is 25 μm SiO₂ + 1 mm Cu and figure 2b is 4 μm Al/1 μm Ni/1 μm CH.

The bright feature in figure 2a corresponds to self emission produced where the laser interacts with the target front surface. The laser is incident from the right side of the image.

The expansion velocities were calculated from the shadowgrams, using the knowledge of the original target surface position and the time that shadowgram was recorded. The error in the velocities came from the combined uncertainty of the expansion position and the original target surface position.

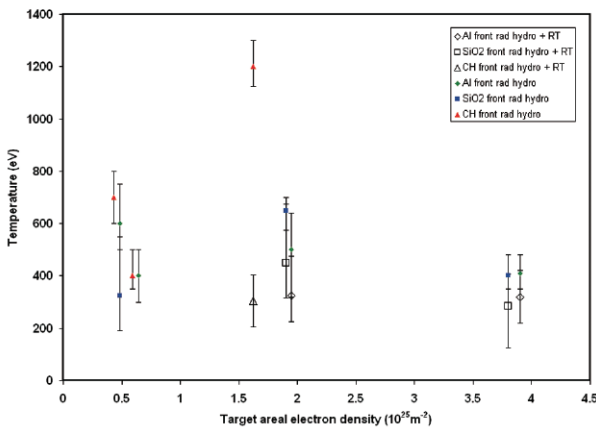


Figure 3. Comparison of rear surface temperatures derived from expansion velocities (measured from shadowgraphy) using HYADES alone (colour) and HYADES with RT model (black) models.

The lateral scale of the expansion for the 25 μm SiO₂ target is ~100 μm and for the thin layered target ~200 μm. The longitudinal scale of the expansion for 25 μm SiO₂ target is ~90 μm and for the thin layered target ~265 μm. We know that the images were taken at $t_0 + 200$ ps and so the expansion velocities (depending on thickness) were in the range $2 \times 10^7 \text{ cm/s} - 1 \times 10^8 \text{ cm/s}$.

The next step in the analysis was to use the experimentally derived expansion velocities in conjunction with a radiation hydrodynamics model to derive a temperature gradient.

Radiation hydrodynamics model

The trajectory of the imaged density contour (from the shadowgraphy) is matched to the predictions of radiation hydrodynamics simulations to obtain an estimate of the bulk temperature attained in each target. HYADES^[9] is a one dimensional Lagrangian radiation hydrodynamics simulation code with multi-group radiation diffusion and a flux limited diffusion model of electron conduction.

In these simulations, an average atom LTE ionisation model and tabulated SESAME equation of state data are employed. The targets are given an initial temperature, to mimic the heating of the short pulse, and HYADES then models the cooling and expansion over time. This approach is considered reasonable since the heating is

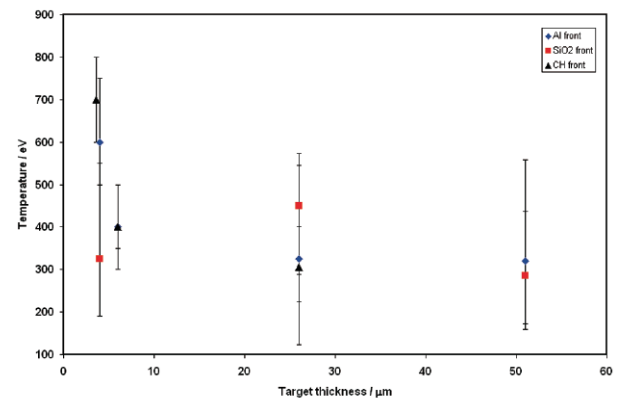


Figure 4. Temperatures from HYADES (with RT model for thick targets with Cu layer) as a function of target thickness.

essentially instantaneous with respect to hydrodynamic timescales. Temperature is iterated to match the observed rear surface trajectory.

Further simulations are performed to match the associated minimum and maximum excursions as dictated by the experimental error bars, as part of the error analysis for temperature.

The thicker targets fielded are expected to be susceptible to the Rayleigh-Taylor fluid instability^[6,7]. The Cu back layer will cool rapidly by radiative emission, and thereafter be pushed by the less dense lower-Z layer beneath it. The interface between the two regions will therefore be Rayleigh-Taylor unstable since the gradient of the pressure is of the opposite sign to the gradient of the density at the boundary. A simple bubble growth model^[8] of the form, $h_b = \alpha A_t a t^2$ in which A_t is the Atwood Number, and α is a scaling constant, is used to estimate the time at which bubbles of the lower-Z material will penetrate through the 1 μm thick Cu back layer.

In such a model the value of α is found from past experiments to be in the range 0.04-0.07; the value of this parameter is therefore assumed to lie in this range, and the effect of the associated uncertainty is incorporated in the error analysis for temperature.

In evaluating the temperature, the copper rear surface layer in the simulation is effectively replaced by the underlying material at the time at which the bubbles are expected to penetrate. The value of acceleration, a , which must be inserted into the growth model to yield the penetration time is estimated on the basis of the experimental results. This is considered reasonable since the expansion of the lighter fluid, once present at the rear surface of the target, will exceed that of the copper.

Discussion

Figure 3 shows the two methods of determining the rear surface temperature plotted against target areal electron density. This value is used instead of thickness to make it easier to compare multiple-material targets. The targets are identified in the legend by the material that the laser interacts with, but the areal density plotted is that of the whole target, including all layers.

The coloured shapes are the simulations without the RT model included. The temperatures for the thick targets with Cu layers on the rear surface (i.e. targets greater than $1.5 \times 10^{25} \text{ m}^{-2}$) produced temperatures that fall outside the upper bounds of previous experimental and theoretical data^[1-4]. This is especially evident in the case of CH with a Cu layer which is a factor ~ 2 -3 higher. The thin target data is in reasonable agreement however.

A simple model for the Rayleigh-Taylor instability was added (as stated in previous section) due to the rapid radiative cooling of the copper compared to the lower Z base material. The thin targets were not expected to be Rayleigh Taylor unstable since the plastic layer at the rear heats up and expands rapidly.

Simulations for the thick targets with Cu layers were repeated using this technique. The open shapes in figure 3

represent the radiation hydrodynamic calculations with RT model included.

Temperatures in the thick targets were reduced to a more reasonable level compared to experimental data/hybrid models, most dramatically the case of CH coated with 1 μm Cu. This demonstrates that failure to combine the RT model with the hydrodynamic calculations for potentially RT unstable boundaries results in the over prediction of rear surface temperature.

Incidentally, the Rayleigh Taylor instability would not be visible in the shadowgrams taken here due to the fact that the ripples are $\sim 1 \mu\text{m}$ and the resolution of our system is greater than this at $\sim 4 \mu\text{m}$.

Figure 4 shows a plot of temperature at the rear surface as a function of total target thickness. The curves are identified by the material on to which the laser is incident. The temperature derived from the radiation hydrodynamics code reach $\sim 700 \text{ eV}$ at 3.5 μm targets down to a value of $\sim 300 \text{ eV}$ at 50 μm . The plastic targets appear to attain the highest temperatures. The temperatures for CH and Al drop to $\sim 400 \text{ eV}$ within 2.4 μm ; a rapid fall with increasing target thickness.

Conclusions

We have shown that it is possible to use a relatively simple method of using shadowgraphy in conjunction with a 1D radiation hydrodynamic model to derive a temperature profile for various types of layered target.

The high Z layer of copper at the rear surface changed the expansion due to radiative effects and the high Z – low Z material boundary was Rayleigh-Taylor unstable. A radiation hydrodynamic model including the effects of the Rayleigh-Taylor instability produced temperatures more closely resembling previously measured temperatures from the same system using X-ray spectroscopy and rear surface optical emission. From this we can conclude that the model is reasonable.

Acknowledgements

The author would like to acknowledge the Vulcan laser staff, engineering staff, and target preparatory staff for all their hard work and assistance in making this experiment possible.

References

1. R.G. Evans *et al.*, *App. Phys. Lett.*, **86**, 191505 (2005).
2. G. Malka *et al.*, *Phys Rev. E*, **77**, 026408 (2008).
3. P. Mora *et al.*, *Phys. Fluids* **22** 2300 (1979).
4. N. Motoaki *et al.*, *New Journal Phys.*, **10**, 043046 (2008).
5. HYADES is a commercial product of Cascade Applied Sciences, email Larsen@casinc.com
6. Lord Rayleigh, *Proc. London Math. Soc.* **14**, 170-177 (1883).
7. G. I. Taylor, *Proc. Roy. Soc. A*, **201**, 192-196 (1950).
8. C. L. Gardner, J. Glimm, O. McBryan, R. Menikoff, D. H. Sharop and O. Zhang, *Phys. Fluids*, **31**, 447 (1988).